

This discussion paper is/has been under review for the journal Hydrology and Earth System Sciences (HESS). Please refer to the corresponding final paper in HESS if available.

Discharge estimation in a backwater affected meandering river

H. Hidayat^{1,2}, B. Vermeulen¹, M. G. Sassi¹, P. J. J. F. Torfs¹, and A. J. F. Hoitink^{1,3}

¹Hydrology and Quantitative Water Management Group, Wageningen University, Wageningen, The Netherlands

²Research Centre for Limnology, Indonesian Institute of Sciences, Cibinong, Indonesia

³Institute for Marine and Atmospheric Research Utrecht, Department of Physical Geography, Utrecht University, Utrecht, The Netherlands

Received: 4 March 2011 – Accepted: 7 March 2011 – Published: 9 March 2011

Correspondence to: H. Hidayat (hidayat.hidayat@wur.nl)

Published by Copernicus Publications on behalf of the European Geosciences Union.

HESSD

8, 2667–2697, 2011

**Discharge in a
backwater affected
river reach**

H. Hidayat et al.

Title Page

Abstract

Introduction

Conclusions

References

Tables

Figures

◀

▶

◀

▶

Back

Close

Full Screen / Esc

Printer-friendly Version

Interactive Discussion



Abstract

Variable effects of backwaters complicate the development of rating curves at hydro-metric measurement stations. In areas influenced by backwater, single-parameter rating curve techniques are often inapplicable. To overcome this, several authors have advocated the use of an additional downstream level gauge to estimate the longitudinal surface level gradient, but this is cumbersome in a lowland meandering river with considerable transverse surface level gradients. Recent developments allow river flow to be continuously monitored through velocity measurements with an acoustic Doppler current profiler (H-ADCP), deployed horizontally at a river bank. This approach was adopted to obtain continuous discharge estimates at a cross-section in the River Mahakam at a station located about 300 km upstream of the river mouth in the Mahakam delta. The discharge station represents an area influenced by variable backwater effects from lakes, tributaries and floodplain ponds, and by tides. We applied both the standard index velocity method and a recently developed methodology to obtain a continuous time-series of discharge from the H-ADCP data. Measurements with a boat-mounted ADCP were used for calibration and validation of the model to translate H-ADCP velocity to discharge. As a comparison with conventional discharge estimation techniques, a stage-discharge relation using Jones formula was developed. The discharge rate at the station exceeded $3300 \text{ m}^3 \text{ s}^{-1}$. Discharge series from a traditional stage-discharge relation did not capture the overall discharge dynamics, as inferred from H-ADCP data. For a specific river stage, the discharge range could be as high as $2000 \text{ m}^3 \text{ s}^{-1}$, which is far beyond what could be explained from kinematic wave dynamics. Backwater effects from lakes were shown to be significant, whereas the river-tide interaction may impact discharge variation in the fortnightly frequency band. Fortnightly tides cannot easily be isolated from river discharge variation, which features similar periodicities.

Discharge in a backwater affected river reach

H. Hidayat et al.

Title Page

Abstract

Introduction

Conclusions

References

Tables

Figures



Back

Close

Full Screen / Esc

Printer-friendly Version

Interactive Discussion



1 Introduction

Discharge is the phase in the hydrological cycle in which water is confined in channels, allowing for an accurate measurement compared to other hydrological phases (Herschy, 2009). Reliable discharge data is vital in research focusing on a broad range of topics related to water management, including water allocation, navigation, and the prediction of floods and droughts. Also, it is crucial in catchment-scale water balance evaluations. Hydrological studies relying on rainfall-runoff models require continuous discharge series for model calibration and validation (e.g. Beven, 2001; McMillan et al., 2010).

Discharge estimates are conventionally obtained from a rating curve model, using water level data as input, and a limited number of discharge measurements for calibration. Despite a number of techniques available to account for unsteady flow conditions, water agencies often assume an unambiguous relation between stage and discharge. Both steady and unsteady rating curve models are prone to uncertainties, related to interpolation and extrapolation error and seasonal variations of the state of the vegetation (Di Baldassarre and Montanari, 2009). Changes in the stage-discharge relations frequently occur due to variable backwater effects, rapidly changing discharge, overbank flow, and ponding in areas surrounding the channel (Herschy, 2009). From discharge uncertainty assessment for the River Po, Di Baldassarre and Montanari (2009) showed that the use of a rating curve can lead to error in discharge estimates averaging 25.6%. In this contribution we show that error in estimates from traditional single gauge rating curves can be even higher, confirming the need for alternative approaches.

Single-valued rating curves can produce biased discharge estimates, especially in highly dynamic rivers and streams. In terms of the momentum equation, this bias is the result of temporal and spatial acceleration terms, and the pressure gradient term, which all have to be neglected to justify an unambiguous relation between stage and discharge. River waves featuring such unambiguous relation are termed kinematic. When the pressure gradient term is retained, but the acceleration terms can be neglected, the

HESSD

8, 2667–2697, 2011

Discharge in a backwater affected river reach

H. Hidayat et al.

Title Page

Abstract

Introduction

Conclusions

References

Tables

Figures



Back

Close

Full Screen / Esc

Printer-friendly Version

Interactive Discussion



momentum balance appears as a convection-diffusion equation that can be solved to yield a non-inertial wave as a special type of diffusion wave (Yen and Tsai, 2001). Several formulas have been developed aiming to obtain discharge from parameters that can readily be derived from water level time-series. Among these, the Jones formula is the most well-known, in which the surface level gradient term is approximated using the kinematic wave equation.

Variable backwater is one of the principle factors that cause an ambiguous stage-discharge relation. Backwater from one or several downstream elements such as tributaries, lakes, ponds or dams, complicates rating curve development at hydrometric gauging stations (Petersen-Overleir and Reitan, 2009), causing curved longitudinal surface level profiles for a constant and uniform river discharge. Tides superimposed on river discharge can produce subtidal water level variations (Buschman et al., 2009), with periods of a fortnight or longer, which may not immediately be recognized as phenomena controlled by the tidal motion. Potentially, water level setup by river-tide interactions can cause backwater effects beyond the point of tidal extinction (Godin and Martínez, 1994).

Recently, approaches have been developed to account for backwater effects, using a twin gauge approach to obtain estimates of the longitudinal water level gradient. Such ratings are developed based on records of stage at a base gauge and the fall of the water surface between the base gauge and a second gauge downstream (Hersch, 2009). Considering the water level gradient to be a known variable and with the assumption of a steady state, the terms representing the pressure gradient and spatial acceleration in the momentum equation can be resolved (Dottori et al., 2009). The application of formulas using simultaneous stage measurements was criticised by Koussis (2010). Dottori and Todini (2010) refuted most of the criticism by Koussis (2010), but acknowledged that in lowland areas with a small bed level gradient, the occurring water level gradient can drop below the measuring accuracy of the level gauge. Dottori and Todini (2010) estimate the minimum distance between the gauges to be in between 2000 and 5000 m when the bed slope is 1×10^{-5} . Neither Koussis (2010)

Discharge in a backwater affected river reach

H. Hidayat et al.

Title Page

Abstract

Introduction

Conclusions

References

Tables

Figures

◀

▶

◀

▶

Back

Close

Full Screen / Esc

Printer-friendly Version

Interactive Discussion



nor Dottori and Todini (2010) considered an additional drawback that arises from lateral water level gradients, which can be considerable especially in meandering rivers characterised by a high sinuosity. In high-curvature river reaches, level gauges on opposite sides of each of the two cross-section would be needed to infer the longitudinal water surface gradient. We conclude that the twin gauge approach to discharge measurements is suboptimal in lowland meandering rivers, which are most susceptible to backwater effects.

Discharge can be estimated from flow velocity, which bears a much stronger relation to discharge than the water surface. Gordon (1989) was among the first to estimate discharge from a boat-mounted acoustic Doppler current profiler (ADCP), which soon after became a standard means of estimating discharge accurately. ADCP surveys are costly and are carried out merely occasionally. Recent developments allow horizontal profiles of flow velocity to be continuously monitored by a horizontal acoustic Doppler current profiler (H-ADCP). The H-ADCP is typically deployed at a river bank, measuring a horizontal velocity profile across a channel. The acquired data can then be used to estimate discharge, predicting cross-section integrated velocity from the array data of flow velocity.

Several methods are available to convert H-ADCP data to discharge. In the Index Velocity Method (IVM), H-ADCP velocity estimates are averaged and regressed directly against discharge from boat-mounted ADCP measurements (Simpson and Bland, 2000). Nihei and Kimizu (2008) adopted a deterministic approach, assimilating H-ADCP data with a two-dimensional model of the velocity distribution over a river cross-section. In the velocity profile method (VPM) described by Le Coz et al. (2008), total discharge is inferred from theoretical vertical velocity profiles, made dimensional with the H-ADCP velocity measurements across the section, extrapolated over the river width. Hoitink et al. (2009) combined elements of the IVM and VPM methods, using a boundary layer model to calculate specific discharge from a point measurement of velocity, and a regression model to relate specific discharge to total discharge. Sassi et al. (2011) elaborated on the work of Hoitink et al. (2009) by embedding a more

**Discharge in a
backwater affected
river reach**

H. Hidayat et al.

Title Page

Abstract

Introduction

Conclusions

References

Tables

Figures



Back

Close

Full Screen / Esc

Printer-friendly Version

Interactive Discussion



sophisticated boundary layer model that accounts for side wall effects in the methodology, and letting model coefficients be stage dependent instead of constant. Whereas both Hoitink et al. (2009) and Sassi et al. (2011) focused on tidal rivers, the present contribution presents an H-ADCP deployment in a backwater affected inland river.

The remainder of this paper is organized as follows. Section 2 describes the field site and data gathering. Section 3 presents flow structure and the techniques adopted to convert H-ADCP velocity data to total discharge, applying the method by Sassi et al. (2011). Also, traditional rating curve techniques used for comparison are described. Section 4 presents the results and a discussion and in Sect. 5 conclusions are drawn.

2 Study area and data gathering

This study is based on measurements carried out in the River Mahakam, which drains an area of about 77 100 km² in East Kalimantan, Indonesia. The H-ADCP measurement station is located in Melak in the middle Mahakam area about 300 km from the delta apex (Fig. 1). The middle Mahakam area is an extremely flat tropical lowland with some thirty shallow lakes connected to the Mahakam through small channels. It can be considered a remote, poorly gauged region. A tributary, River Kedang Pahu, meets the Mahakam about 30 km downstream of Melak. Downstream of the lakes region, the Mahakam is tied to three other main tributaries (River Belayan, Kedang Kepala, and Kedang Rantau) and flows south-eastwards until the discharge is divided over delta distributaries debouching into the Makassar Strait.

The H-ADCP discharge measurement station was operational at a 250 m wide cross section of the Mahakam river in Melak (Fig. 2) between March 2008 and August 2009. A 600 kHz H-ADCP manufactured by RD Instruments was mounted on a solid jetty in the concave side of the river bend. Riverbanks at this particular location are quite steep, leading to a cross-section with a relatively confined flow, except at very high and unusual discharges. The H-ADCP was mounted at about 2.5 m below the lowest recorded water level and about 2 m from the bottom. Pitch and roll of the instrument

Discharge in a backwater affected river reach

H. Hidayat et al.

Title Page

Abstract

Introduction

Conclusions

References

Tables

Figures



Back

Close

Full Screen / Esc

Printer-friendly Version

Interactive Discussion



remained relatively constant during the measuring period, amounting to 0.3° and 0.01° , respectively. The measurement protocol for the H-ADCP consisted in 10 min bursts at 1 Hz every 30 min.

The H-ADCP used in this study is a three-beam instrument with angles between beams of 25° and an acoustic beam width ϕ of 1.2° . The H-ADCP was installed at a distance $d = 7.9$ m below the mean water level, with the transducer head at $x = 74.4$ m from the shore. Because the H-ADCP was deployed looking slightly upward, the H-ADCP measured a volume-averaged velocity at elevation z_c , which is calculated from:

$$z_c = \begin{cases} -d + \tan(\theta)(n-x) & \text{if } d + \eta > \tan(\phi/2 + \theta)(n-x) \\ -d + \tan(\theta)(n-x) + \Delta z & \text{otherwise} \end{cases} \quad (1)$$

where θ is pitch, n is cross-channel coordinate, with the origin at the river bank and η is water level variation. Δz is the level difference between the centroid of the ensonified water area and the central beam axis. This correction accounts for the lowering of the centroid of the ensonified water volume if the main lobe intersects with the water surface at low water (Hoitink et al., 2009).

Conventional boat-mounted ADCP measurements were periodically taken at the cross-section where the H-ADCP was deployed to establish water discharge through the river section. Eight campaigns were carried out spanning low and high flow conditions. The campaign consisted of transects in front of the H-ADCP for determining hydraulic parameters (referred to as “par”) and transects carried out about 20 m upstream to cover the whole river section for calibrating the discharge computation (referred to as “cal”). Each transect measurement spanned over about two hours. The boat was equipped with a 1.2 MHz RDI Broadband ADCP measuring in mode 12, a DGPS compass and an echosounder. The ADCP measured a single ping ensemble at approximately 1 Hz with a depth cell size of 0.35 m. Each ping was composed of 6 sub-pings, separated by 0.04 s. The range to the first cell center was 0.865 m. The boat speed ranged between 1 and 3 m s^{-1} .

Discharge in a backwater affected river reach

H. Hidayat et al.

Title Page

Abstract

Introduction

Conclusions

References

Tables

Figures

◀

▶

◀

▶

Back

Close

Full Screen / Esc

Printer-friendly Version

Interactive Discussion



Depth estimates from the ADCP bottom pings were used to construct a local depth map. The range estimation from the four acoustic beams was corrected for pitch, roll, and heading of the ADCP, and referenced to the mean water level. Bathymetry data were also collected using a single beam echosounder for validation. Water levels were measured using pressure transducers in Melak at the H-ADCP station, in Lake Jempang, and in Muara Kaman at the confluence of River Kedang Rantau with the Mahakam, downstream of the Makaham lakes area.

3 Methods to estimate discharge

3.1 Flow structure

The design of an appropriate discharge estimation method requires information about the local flow structure, which is discussed in the present section based on the boat-mounted ADCP surveys. The ADCP velocity measurements were projected into normalized (β, σ) coordinates. The normalized spanwise coordinate β was obtained by normalizing the distance from the bank to the maximum width within that survey. The normalized vertical coordinate σ was obtained from:

$$\sigma = \frac{H + z}{H + \eta} \quad (2)$$

where H is water depth, z is normal distance from the bed. The mesh size of the coordinate was $\Delta\beta = 0.025$ and $\Delta\sigma = 0.05$. Turbulence fluctuations were removed by taking the mean over the repeated velocity recordings for each grid cell within a survey. Velocity profiles from boat-mounted ADCP measurements were then averaged over

Discharge in a backwater affected river reach

H. Hidayat et al.

Title Page

Abstract

Introduction

Conclusions

References

Tables

Figures



Back

Close

Full Screen / Esc

Printer-friendly Version

Interactive Discussion



3.2 Semi-deterministic semi-stochastic method

In the semi-Deterministic semi-Stochastic Model (DSM) developed by Hoitink et al. (2009) and Sassi et al. (2011), time-series of single point velocity u_c , measured at the relative height σ_c , are translated into depth-mean velocity U according to:

$$U = F u_c \quad (5)$$

where

$$F = \frac{\ln\left(\frac{H}{\exp(1+\alpha)}\right) - \ln(z_0)}{\ln(\sigma_c H) + \alpha \ln(1 - \sigma_c) - \ln(z_0)} \quad (6)$$

Herein, α accounts for sidewall effects that retard the flow near the surface by means of secondary circulations and z_0 is the apparent roughness length. The value of α is obtained from:

$$\alpha = \frac{1}{\sigma_{\max}} - 1 \quad (7)$$

where σ_{\max} is the relative height where the maximum velocity occurs. To estimate σ_{\max} we closely followed the approach of Sassi et al. (2011) by repeatedly fitting a logarithmic profile starting with the lowermost three ADCP cells, adding successively a velocity cell from the bottom to the top for each fit. σ_{\max} is determined from the development of the goodness of fit which decreases once the cell above σ_{\max} is included. Figure 5 illustrates that cross-river profiles of α do not show a systematic variation between $0.2 < \beta < 0.9$. We adopt a constant value of $\alpha = 0.28$, which results in $\sigma_{\max} = 0.78$.

The determination of the effective hydraulic roughness length z_0 is fundamental in the approaches by both Hoitink et al. (2009) and Sassi et al. (2011). The value of z_0 is obtained as:

$$z_0 = \frac{H}{\exp\left(\frac{\kappa U}{u_*} + 1 + \alpha\right)} \quad (8)$$

where κ is the Von Karman constant and u_* is the shear velocity. Values of u_* coincide with the slope of the linear regression line of $u(\sigma)$ against $(\ln(\sigma) + 1 + \alpha + \alpha \ln(1 - \sigma)) / \kappa$ (Sassi et al., 2011). Figure 6 shows that values of z_0 change over width and are consistent at each β location for each ADCP campaigns in the range $\beta > 0.4$. The geometric mean of z_0 at each β location over all boat-mounted transects in front of the H-ADCP (par) were taken for further computation, processing only the H-ADCP data in the range $\beta > 0.4$.

Specific discharge q is obtained from $q = UH$, where U is depth mean velocity estimates from H-ADCP measurements. Discharge Q is obtained from:

$$Q(t) = f(\beta)Wq(\beta, t) \quad (9)$$

where W is the river width, $f(\beta)$ is constant amplification factor obtained from the total discharge of each “cal” campaign divided by the product Wq from the “par” campaigns. Profiles of f remain constant up to $\beta = 0.8$ during the two calibration campaigns (Fig. 7). The mean value of f at each β location was taken for discharge computation.

3.3 Index velocity method

We estimated discharge from the H-ADCP data based on the widely used IVM approach (Simpson and Bland, 2000; Le Coz et al., 2008), which is more straightforward than the approach by Sassi et al. (2011). The sectionally integrated velocity obtained from the boat-mounted ADCP is regressed against the width-averaged along channel velocity (i.e. the index velocity) obtained with the H-ADCP. Figure 8 shows the regression results.

Discharge in a backwater affected river reach

H. Hidayat et al.

Title Page

Abstract

Introduction

Conclusions

References

Tables

Figures

◀

▶

◀

▶

Back

Close

Full Screen / Esc

Printer-friendly Version

Interactive Discussion



3.4 Stage-discharge relation

To investigate the degree in which discharge at Melak station can be captured by a rating curve, Jones' formula was applied, which reads:

$$Q = Q_{\text{kin}} \left\{ 1 + \frac{1}{cS_0} \frac{\partial h}{\partial t} \right\}^{1/2} \quad (10)$$

where Q_{kin} is the kinematic discharge, c is wave celerity, S_0 is bed slope, and $\partial h/\partial t$ is rate of water level change in time t (Petersen-Overleir, 2006). The celerity c was estimated from $c = \sqrt{gd}$ (Liggett and Langley, 1998), where g is gravitational acceleration and d is hydraulic mean depth, according to $d = A/b$. Herein, A is river cross sectional area and b is river width. The bed slope was estimated from the Mahakam River bed level profile derived from SRTM data by van Gerven and Hoitink (2009). Q_{kin} was calculated by Manning formula:

$$Q_{\text{kin}} = \frac{1}{n} S_0^{1/2} AR^{2/3} \quad (11)$$

where n is Manning roughness coefficient, R is hydraulic radius obtained from the ratio between A and the wetted perimeter of the river cross-section. The Manning coefficient was estimated based on an evaluation of the river geometry and composition, following a standard empirical technique provided by Gore (2006). The details of channel evaluation to determine n are presented in Table 1.

4 Results and discussion

Table 2 shows the validation results. Discharge estimates obtained by applying the method by Sassi et al. (2011) differed less than 5% from the accurate estimates obtained from the boat surveys, whereas discharge estimates from the IVM feature a bias

up to 23%. Figure 9 shows time-series of the absolute and relative difference between Q_{DSM} and Q_{IVM} , which indicate that the validation results represent the medium to high flows well. During low flows, Q_{DSM} and Q_{IVM} can deviate much more, both in a relative and in an absolute sense. Unfortunately, a planned validation survey during the low flow was cancelled due to technical problems, which could have shed more light on the validity of the low-flow discharge estimates. Regarding the medium to high flows, the larger bias introduced by the index velocity method is due to the fact that the H-ADCP is monitoring flow at a relative depth that changes with the river stage, which challenges the constancy of the conversion factor to calculate discharge from the index velocity. The obtained results highlight the merits of applying the more elaborate procedure advocated by Hoitink et al. (2009) and Sassi et al. (2011), which in this case reduces the difference with the reference measurements from typically 20% to less than 5%.

H-ADCP measurements at Melak station revealed a complex stage-discharge relation that was highly hysteretic (Fig. 10). Hysteresis is generally related to flood wave propagation. For the same water level, higher discharge during rising stage and lower discharge during falling stage are known to occur, resulting in distinctive loops in stage-discharge relationships (Petersen-Overleir, 2006). At Melak station, the range of discharges that can occur for a specific stage can span over more than $2000 \text{ m}^3 \text{ s}^{-1}$, which is exceptionally large in comparison with the maximum discharge of $3370 \text{ m}^3 \text{ s}^{-1}$. Such variation can be considered far beyond the rising stage and falling stage explanation. Compared to standard rating curves for different hydraulic conditions (Hersch, 2009), the stage-discharge relation in Fig. 10 will reflect the presence of variable backwater effects, looping due to changing discharge, and multiple looping due to overbank flow and ponding. Radar images showed vast areas in the Mahakam Lakes Region to become inundated during high flows (Hidayat et al., 2011). Part of the complexity in the stage-discharge relation can be explained from the subharmonics generated by river-tide interactions (Buschman et al., 2009). At low discharges in August 2009, the tidal signal is clearly visible in the discharge series. Due to the flat terrain of the middle and lower Mahakam, tidal energy propagates up to the Mahakam lakes area, where much

**Discharge in a
backwater affected
river reach**

H. Hidayat et al.

Title Page

Abstract

Introduction

Conclusions

References

Tables

Figures

◀

▶

◀

▶

Back

Close

Full Screen / Esc

Printer-friendly Version

Interactive Discussion



of the tidal energy is dissipated. Subharmonics such as the fortnightly tide MS_f may extend beyond the lakes region, but cannot be readily isolated from river discharge variation as discharge variation features fortnightly variation both in the presence and in absence of a tidal influence.

5 The wide loops in the stage-discharge plots are the result of the geographical complexity of the region where Melak station is located, experiencing a flashy discharge from upstream and backwater effects from downstream. The flashy discharge regime relates to high rainfall rates in large parts of the catchment upstream of Melak, which dominates the moderating effect of the rain forest. The backwater effects are caused
10 both by the lakes and a number of tributaries, all affecting the water level profile. Lake emptying and filling processes contribute to retarding and accelerating the river flow velocity. Figure 11 illustrates the lake emptying and lake filling influencing water levels and discharge upstream. At the start of lake emptying, when the lake level was still high, water stage in Melak was relatively high for a relatively low discharge. When the
15 lake level dropped, the backwater effect was reduced and discharge increased while water stage kept decreasing until the point that discharge was sufficiently high to make water stage follow the trend in the discharge time-series. The opposite mechanism took place during lake filling as shown in Fig. 11 (bottom panel). Water stage records downstream of the Mahakam lake area (Muara Kaman) indicate that some peaks of
20 water level were shaved by the lake filling and emptying mechanism.

The discharge obtained from the stage-discharge relation using Jones formula is merely a rough estimate of discharge at Melak station, indicating the range of discharge variation. It did not capture the detailed discharge dynamics as revealed by the H-ADCP measurements. This can be related to a wide variety of reasons. The
25 Froude number takes a value around 0.01, which legitimizes neglecting the spatial and temporal acceleration terms in the momentum equation, validating the non-inertial wave approximation. The key assumption used to derive the Jones formula is the applicability of the kinematic wave equation to deal with the surface gradient term in the non-inertial wave equation. There is no theoretical justification for this, and it is

**Discharge in a
backwater affected
river reach**

H. Hidayat et al.

Title Page

Abstract

Introduction

Conclusions

References

Tables

Figures



Back

Close

Full Screen / Esc

Printer-friendly Version

Interactive Discussion



well-known that the kinematic wave equation cannot capture discharge dynamics in a backwater effected river reach (e.g. Tsai, 2005). The Jones formula is just one of a series of formulas available to predict discharge from time-series of a single level gauge (Henderson, 1966; Di Silvio, 1969; Fread, 1975; Lamberti and Pilati, 1990; Perumal and Ranga Raju, 1999), all aiming to improve the original Jones' formula. Dottori et al. (2009) systematically reviewed those formulas, explicitly mentioning they are best applicable when flow conditions are quasi kinematic. None of these approaches will be capable of reproducing the wide loops occurring at Melak station, which underlines the importance of monitoring additional information besides stage at a single section. Considering the ease of deployment of H-ADCPs, they are a promising alternative to the dual gauge approach advocated by a.o. Dottori et al. (2009).

5 Conclusions

Flow measurements using a 600 kHz H-ADCP were carried out at a 300 m wide cross section of the Mahakam River in Melak, 40 km upstream of the Mahakam lakes area. Conventional boat-mounted ADCP measurements were periodically taken to establish water discharge through the cross section. We followed a recently developed semi-deterministic, semi-stochastic method to convert the H-ADCP to discharge, and compared the results with those obtained from the standard index-velocity method and a rating curve model. The new method was found to reduce the difference with discharge estimates from the boat-mounted ADCP surveys from around 20% to less than 5%, based on three validation surveys. The continuous time-series of discharge showed that the validation data were representative for medium to high flows. A stage-discharge model based on Jones's formula captured only a small portion of the discharge dynamics, which was attributed to the invalidity of the kinematic wave assumption. A discharge range of about $2000 \text{ m}^3 \text{ s}^{-1}$ was established for a particular stage in the recorded discharge series, which is about 60% of the peak discharge and therefore exceptionally large. The large range of discharge occurring for a given stage was

Discharge in a backwater affected river reach

H. Hidayat et al.

Title Page

Abstract

Introduction

Conclusions

References

Tables

Figures



Back

Close

Full Screen / Esc

Printer-friendly Version

Interactive Discussion



attributed to multiple backwater effects from lakes and tributaries, floodplain impacts and effects of river-tide interaction, which generate subharmonics that cannot readily be isolated from river discharge oscillations.

Acknowledgements. This research has been supported by the Netherlands organisation for scientific research, under grant number WT 76-268. The help from Fajar Setiawan and Unggul Handoko (LIPI – Research Centre for Limnology) and David Vermaas (Wageningen University) in data collection is gratefully acknowledged.

References

- Beven, K. J.: Rainfall-runoff modelling: the primer, John Wiley & Sons, Chichester, England, 2001. 2669
- Buschman, F. A., Hoitink, A. J. F., van der Vegt, M., and Hoekstra, P.: Subtidal water level variation controlled by river flow and tides, *Water Resour. Res.*, 45, 1–12, doi:10.1029/2009WR008167, 2009. 2670, 2679
- Di Baldassarre, G. and Montanari, A.: Uncertainty in river discharge observations: a quantitative analysis, *Hydrol. Earth Syst. Sci.*, 13, 913–921, doi:10.5194/hess-13-913-2009, 2009. 2669
- Di Silvio, G.: Flood wave modifications along prismatic channels, *J. Hydraul. Div. ASCE*, 95, 1589-1614, 1969. 2681
- Dottori, F. and Todini, E.: Reply to Comment on “A dynamic rating curve approach to indirect discharge measurement by Dottori et al. (2009)” by Koussis (2009), *Hydr. Earth Syst. Sc.*, 14, 1099–1107, doi:10.5194/hess-14-1099-2010, 2010. 2670, 2671
- Dottori, F., Martina, M. L. V., and Todini, E.: A dynamic rating curve approach to indirect discharge measurement, *Hydrol. Earth Syst. Sci.*, 13, 847–863, doi:10.5194/hess-13-847-2009, 2009. 2670, 2681
- Fread, D. L.: Computation of stage-discharge relationship affected by unsteady flow, *Water Resour. Bull.*, 12, 429-442, 1975. 2681
- Godin, G. and Martínez, A.: Numerical experiments to investigate the effects of quadratic friction on the propagation of tides in a channel, *Cont. Shelf Res.*, 14, 723–748, 1994. 2670
- Gordon, R. L.: Acoustic measurement of river discharge, *J. Hydraul. Eng.*, 115, 925–936, 1989. 2671

Discharge in a backwater affected river reach

H. Hidayat et al.

Title Page

Abstract

Introduction

Conclusions

References

Tables

Figures

◀

▶

◀

▶

Back

Close

Full Screen / Esc

Printer-friendly Version

Interactive Discussion



Discharge in a backwater affected river reach

H. Hidayat et al.

Title Page

Abstract

Introduction

Conclusions

References

Tables

Figures

◀

▶

◀

▶

Back

Close

Full Screen / Esc

Printer-friendly Version

Interactive Discussion



- Gore, J. A.: Methods in Stream Ecology, chap. Discharge Measurements and Streamflow Analysis, 51–77, Academic Press, 2006. 2678
- Henderson, F. M.: Open channel flow, Prentice Hall, 544 pp., 1966. 2681
- Hersch, R. W.: Streamflow Measurement, Taylor & Francis, London and New York, third edn., 2009. 2669, 2670, 2679
- 5 Hidayat, Hoekman, D. H., Vissers, M. A. M., and Hoitink, A. J. F.: Combining ALOS-PALSAR imagery with field water level measurements for flood mapping of a tropical floodplain, International Symposium on LIDAR and Radar Mapping: Technologies and Applications, Nanjing, China, submitted, 2011. 2679
- 10 Hoitink, A. J. F., Buschman, F. A., and Vermeulen, B.: Continuous measurements of discharge from a horizontal acoustic Doppler current profiler in a tidal river, Water Resour. Res., 45, 1–13, doi:10.1029/2009WR007791, 2009. 2671, 2672, 2673, 2676, 2679
- Koussis, A. D.: Comment on “A praxis-oriented perspective of streamflow inference from stage observations - the method of Dottori et al. (2009) and the alternative of the Jones Formula, with the kinematic wave celerity computed on the looped rating curve” by Koussis (2009), Hydrol. Earth Syst. Sci., 14, 1093-1097, doi:10.5194/hess-14-1093-2010, 2010. 2670
- 15 Lamberti, P. and Pilati, S.: Quasi-kinematic flood wave propagation, Meccanica, 25, 107–114, 1990. 2681
- Le Coz, J., Pierrefeu, G., and Paquier, A.: Evaluation of river discharges monitored by a fixed side-looking Doppler profiler, Water Resour. Res., 44, 1–13, doi:10.1029/2008WR006967, 2008. 2671, 2677
- 20 Liggett, J. A. and Langley, D. A.: Fluid Mechanics, ASCE Press, 1998. 2678
- McMillan, H., Freer, J., Pappenberger, F., Krueger, T., and Clark, M.: Impacts of uncertain river flow data on rainfall-runoff model calibration and discharge predictions, Hydrol. Process., 24, 1270–1284, doi:10.1002/hyp.7587, 2010. 2669
- 25 Nihei, Y. and Kimizu, A.: A new monitoring system for river discharge with horizontal acoustic Doppler current profiler measurements and river flow simulation, Water Resour. Res., 44, 1–15, doi:10.1029/2008WR006970, 2008. 2671
- Perumal, M. and Ranga Raju, K. G.: Approximate convection-diffusion equations, J. Hydrol. Eng., 4, 160–164, 1999. 2681
- 30 Petersen-Overleir, A.: Modelling stage-discharge relationships affected by hysteresis using the Jones formula and nonlinear regression, Hydrol. Sci. J., 51, 365–388, 2006. 2678, 2679
- Petersen-Overleir, A. and Reitan, T.: Bayesian analysis of stage-fall-discharge models

Discharge in a backwater affected river reach

H. Hidayat et al.

Title Page

Abstract

Introduction

Conclusions

References

Tables

Figures

◀

▶

◀

▶

Back

Close

Full Screen / Esc

Printer-friendly Version

Interactive Discussion



for gauging stations affected by variable backwater, *Hydrol. Process.*, 23, 3057–3074, doi:10.1002/hyp.7417, 2009. 2670

Sassi, M. G., Hoitink, A. J. F., Vermeulen, B., and Hidayat: Discharge estimation from H-ADCP measurements in a tidal river subject to sidewall effects and a mobile bed, *Water Resour. Res.*, in press, available at: <http://www.agu.org/journals/wr/papersinpress.shtml>, 2011. 2671, 2672, 2675, 2676, 2677, 2678, 2679

Simpson, M. R. and Bland, R.: Methods for accurate estimation of net discharge in a tidal channel, *IEEE J. Oceanic Eng.*, 25, 437–445, 2000. 2671, 2677

Tsai, C. W.: Flood routing in mild-sloped rivers – wave characteristics and downstream backwater effect, *J. Hydrol.*, 308, 151–167, doi:10.1016/j.jhydrol.2004.10.027, 2005. 2681

van Gerven, L. P. A. and Hoitink, A. J. F.: Analysis of river planform geometry with wavelets: application to the Mahakam River reveals geographical zoning, in: *Proceedings of RCEM*, 2009. 2678

Yen, B. C. and Tsai, C. W. S.: On noninertia wave versus diffusion wave in flood routing, *J. Hydrol.*, 244, 97–104, 2001. 2670

Discharge in a backwater affected river reach

H. Hidayat et al.

Table 1. Evaluation of channel conditions at Melak station to estimate the Manning coefficient.

Factor (index)	Description (value)
Additive factors	
– Material involved (n_0)	Earth (0.02)
– Degree of irregularity (n_1)	Minor (0.005)
– Var. in location of thalweg (n_2)	Gradual (0.00)
– Effect of obstruction (n_3)	Negligible (0.00)
– Riparian vegetation (n_4)	Medium (0.01)
Multiplicative factors	
– Degree of meandering (m)	Appreciable (1.15)
$n = (n_0 + n_1 + n_2 + n_3 + n_4)m = 0.04025$	

Title Page

Abstract

Introduction

Conclusions

References

Tables

Figures

◀

▶

◀

▶

Back

Close

Full Screen / Esc

Printer-friendly Version

Interactive Discussion



Discharge in a backwater affected river reach

H. Hidayat et al.

Table 2. Results of the three validation surveys of the DSM and IVM methods. Q_{BS} denotes the discharge calculated from the boat survey, which can be considered truth.

Validation survey	Q_{BS}	Q_{DSM}	Q_{IVM}	Q_{DSM}/Q_{BS}	Q_{IVM}/Q_{BS}
1	1823	1897	2241	1.04	1.23
2	2438	2445	2924	1.00	1.20
3	2387	2437	2857	1.02	1.20

Title Page

Abstract

Introduction

Conclusions

References

Tables

Figures

◀

▶

◀

▶

Back

Close

Full Screen / Esc

Printer-friendly Version

Interactive Discussion



**Discharge in a
backwater affected
river reach**

H. Hidayat et al.

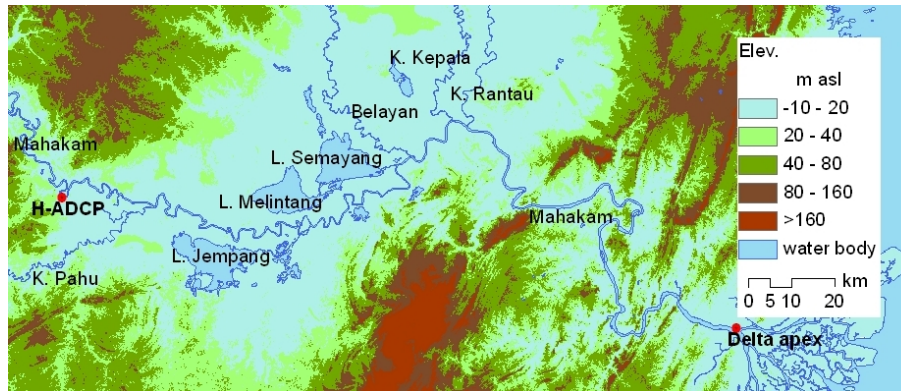


Fig. 1. Location of H-ADCP discharge station in the Mahakam River, plotted on a digital elevation model obtained from Shuttle Radar Topographic Mission (SRTM) data.

[Title Page](#)[Abstract](#)[Introduction](#)[Conclusions](#)[References](#)[Tables](#)[Figures](#)[◀](#)[▶](#)[◀](#)[▶](#)[Back](#)[Close](#)[Full Screen / Esc](#)[Printer-friendly Version](#)[Interactive Discussion](#)

Discharge in a
backwater affected
river reach

H. Hidayat et al.

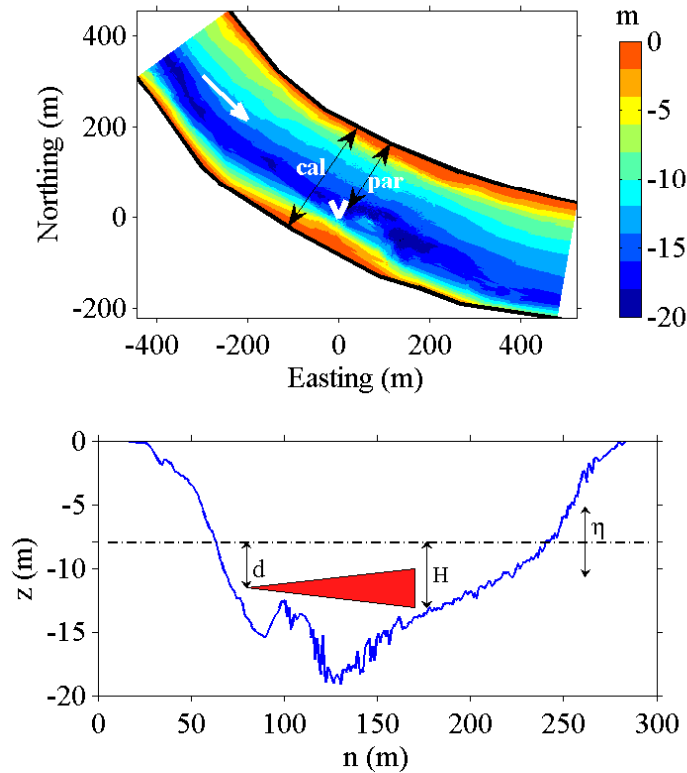


Fig. 2. Top: bathymetry at Melak discharge gauging station. The arrow indicates flow direction, V indicates the location where the H-ADCP was deployed, double arrows indicate locations of boat-mounted ADCP transects. Bottom: channel cross-sectional profile at the station. The shaded area indicates cross-section of the H-ADCP conical measuring volume.

Title Page

Abstract Introduction

Conclusions References

Tables Figures

◀ ▶

◀ ▶

Back Close

Full Screen / Esc

Printer-friendly Version

Interactive Discussion



Discharge in a backwater affected river reach

H. Hidayat et al.

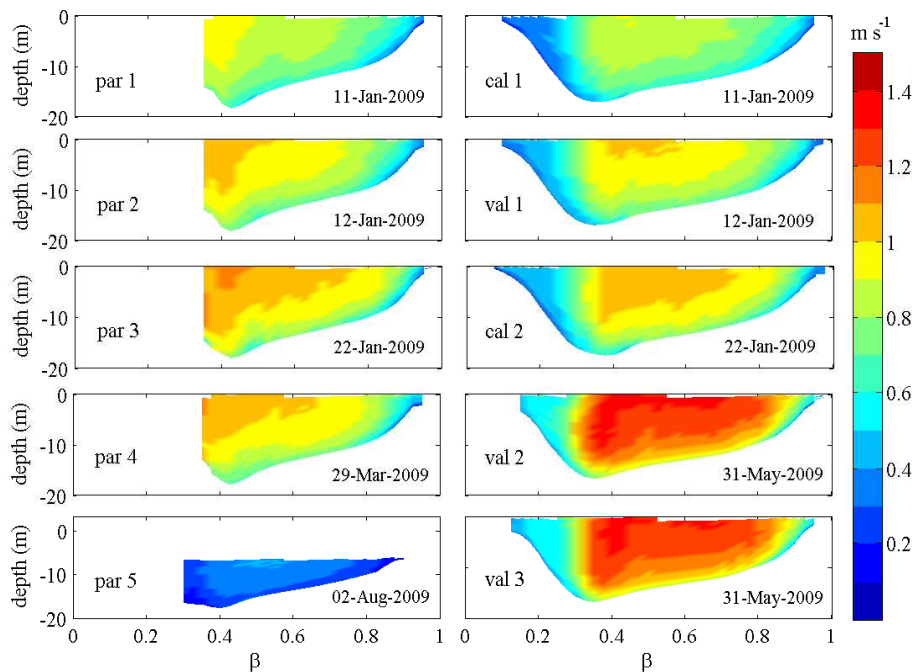


Fig. 3. Streamwise velocity spatial structure over the cross-section during boat-mounted ADCP campaigns. Transects labelled “par” were taken in front of the H-ADCP to obtain hydraulic parameters, while the ones labelled “cal” were taken 20 m upstream to cover the whole channel width for calibration and validation.

Title Page

Abstract

Introduction

Conclusions

References

Tables

Figures

◀

▶

◀

▶

Back

Close

Full Screen / Esc

Printer-friendly Version

Interactive Discussion



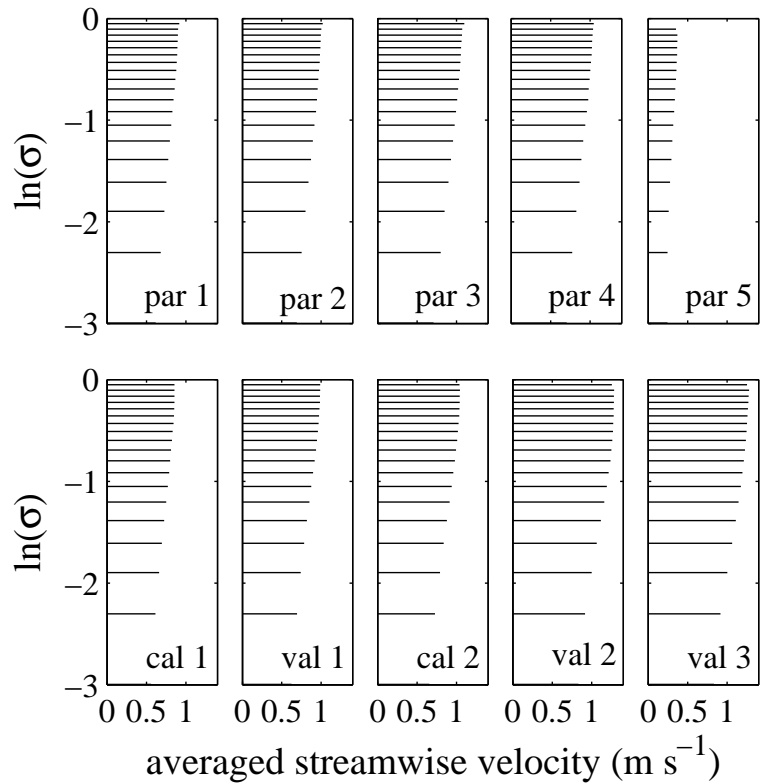


Fig. 4. Velocity profiles averaged over the middle part of the river section ($\beta = 0.35 - 0.65$) during the ADCP campaigns. The length of lines represents velocity magnitude.

Discharge in a backwater affected river reach

H. Hidayat et al.

Title Page

Abstract Introduction

Conclusions References

Tables Figures

◀ ▶

◀ ▶

Back Close

Full Screen / Esc

Printer-friendly Version

Interactive Discussion



Discharge in a backwater affected river reach

H. Hidayat et al.

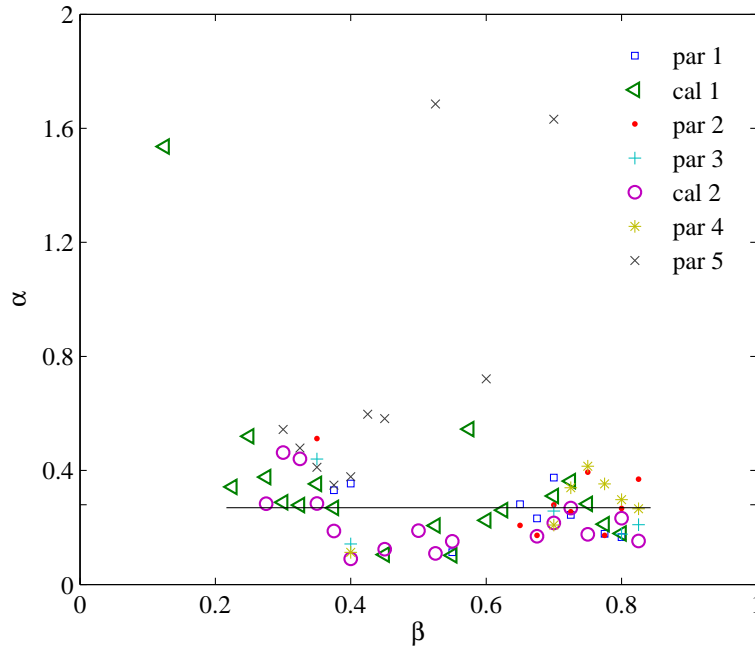


Fig. 5. Profiles of α across the river section for all parameter and calibration surveys. In the conversion model $\alpha = 0.28$ is taken for $\beta > 0.35$.

Title Page

Abstract

Introduction

Conclusions

References

Tables

Figures

◀

▶

◀

▶

Back

Close

Full Screen / Esc

Printer-friendly Version

Interactive Discussion



Discharge in a backwater affected river reach

H. Hidayat et al.

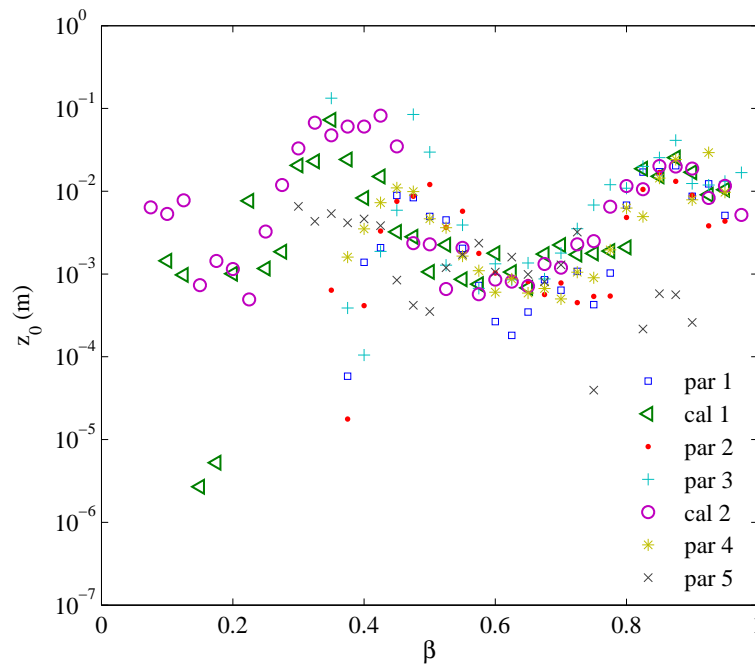


Fig. 6. Cross-river profiles of z_0 for all parameter and calibration surveys.

Title Page

Abstract

Introduction

Conclusions

References

Tables

Figures

◀

▶

◀

▶

Back

Close

Full Screen / Esc

Printer-friendly Version

Interactive Discussion



**Discharge in a
backwater affected
river reach**

H. Hidayat et al.

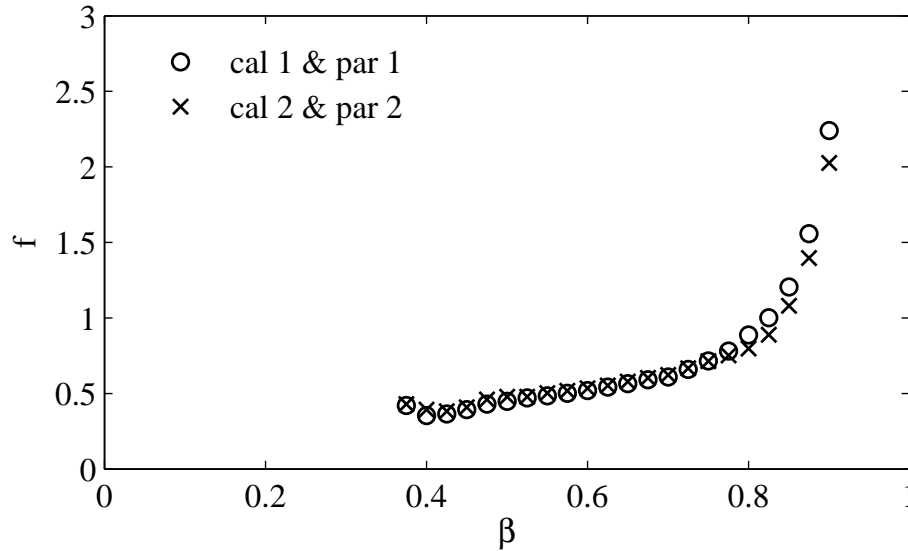


Fig. 7. Amplification factor f obtained for quasi-simultaneous parameter and calibration surveys.

[Title Page](#)[Abstract](#)[Introduction](#)[Conclusions](#)[References](#)[Tables](#)[Figures](#)[◀](#)[▶](#)[◀](#)[▶](#)[Back](#)[Close](#)[Full Screen / Esc](#)[Printer-friendly Version](#)[Interactive Discussion](#)

**Discharge in a
backwater affected
river reach**

H. Hidayat et al.

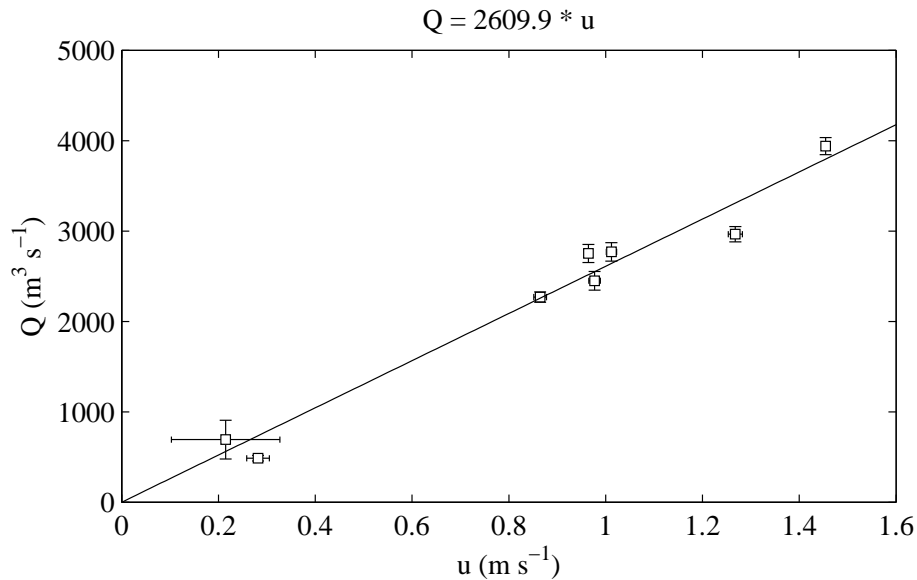


Fig. 8. Discharge (Q) as a function of index velocity (u) measured by the H-ADCP at Melak station. Standard deviations represented by error bars in the plot indicate that flow variations were higher during low flow condition.

Title Page

Abstract

Introduction

Conclusions

References

Tables

Figures

◀

▶

◀

▶

Back

Close

Full Screen / Esc

Printer-friendly Version

Interactive Discussion



Discharge in a backwater affected river reach

H. Hidayat et al.

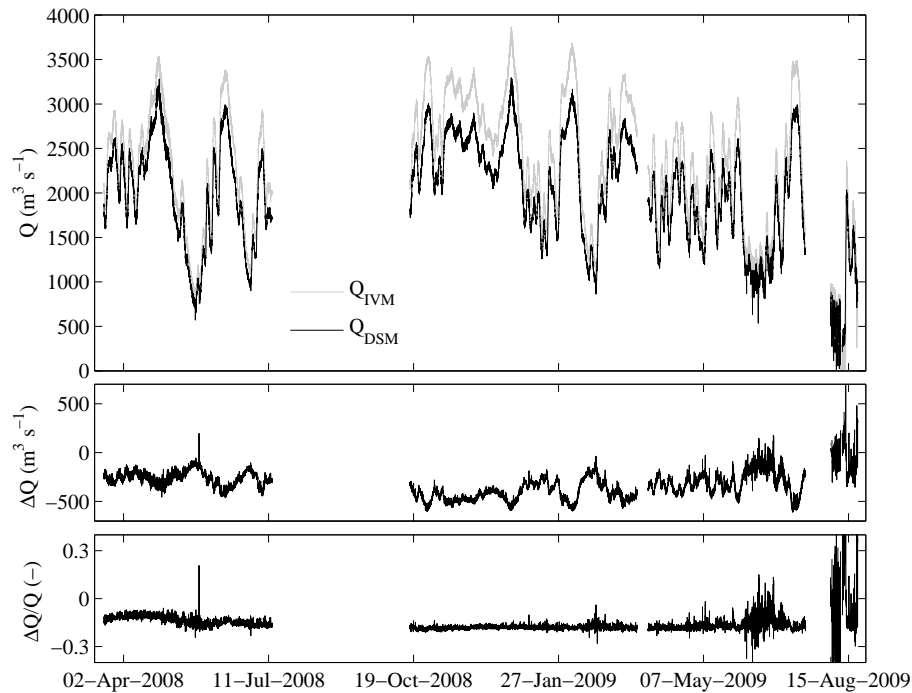


Fig. 9. Continuous series of discharge estimates derived from H-ADCP data with the DSM and the IVM. Central and bottom panels offer a comparison between the two approaches to convert H-ADCP data to discharge, where $\Delta Q = Q_{\text{DSM}} - Q_{\text{IVM}}$.

Title Page

Abstract

Introduction

Conclusions

References

Tables

Figures

◀

▶

◀

▶

Back

Close

Full Screen / Esc

Printer-friendly Version

Interactive Discussion



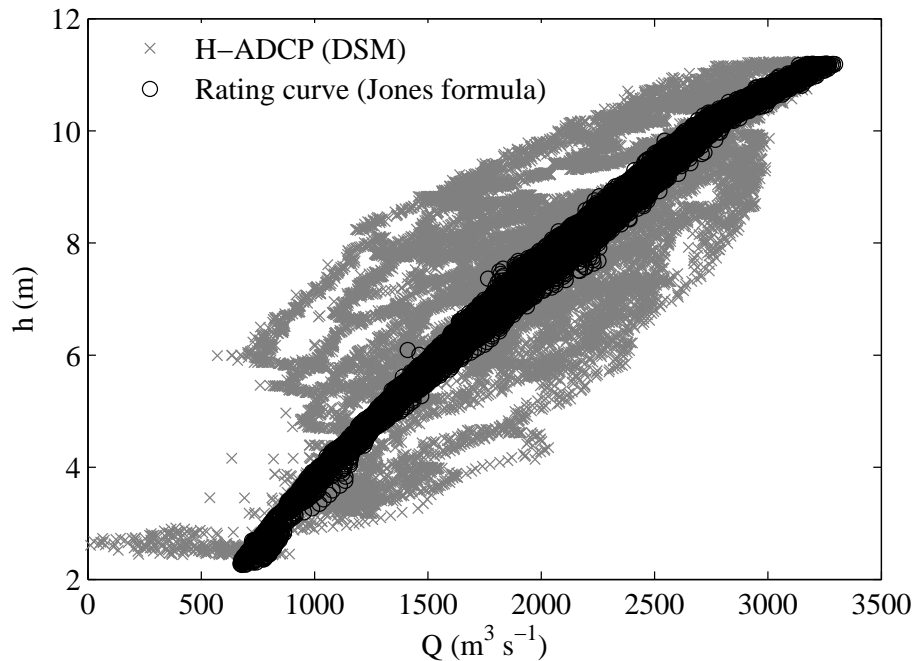


Fig. 10. Water stage and discharge estimates at Melak station, obtained from a rating curve (Jones' formula) and from H-ADCP measurements, applying the DSM. Water stage is with respect to the position of a pressure gauge about 9 m from the deepest part of the river cross-section.

Discharge in a backwater affected river reach

H. Hidayat et al.

Title Page

Abstract

Introduction

Conclusions

References

Tables

Figures

◀

▶

◀

▶

Back

Close

Full Screen / Esc

Printer-friendly Version

Interactive Discussion



Discharge in a backwater affected river reach

H. Hidayat et al.

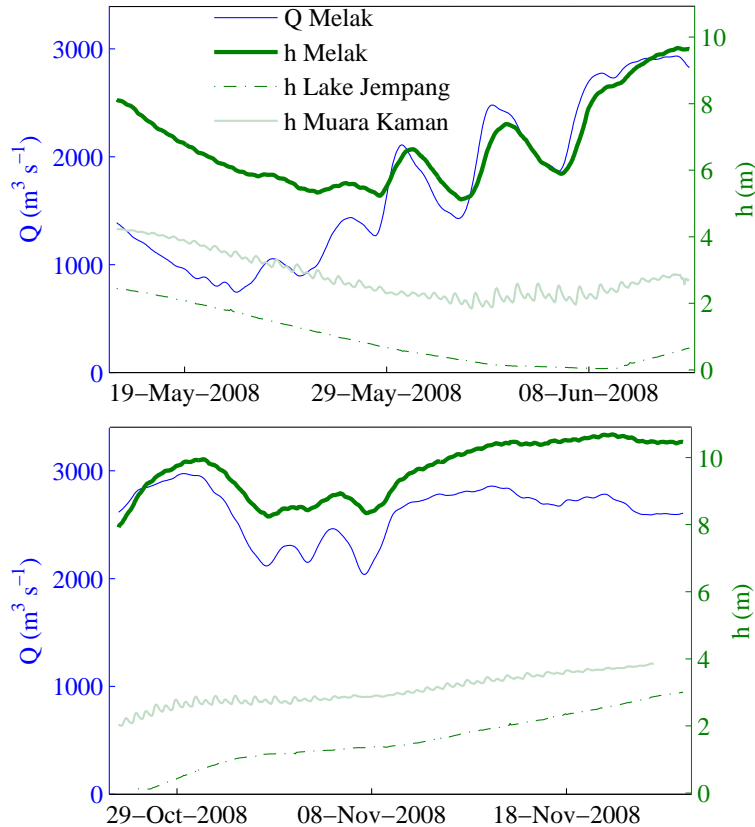


Fig. 11. Water stage and discharge during lake emptying (top) and during lake filling (bottom). Muara Kaman, where the tidal signal was observed during most of the measurement period, is located downstream of the Mahakam lakes area about 170 km from Melak.

[Title Page](#)
[Abstract](#)
[Introduction](#)
[Conclusions](#)
[References](#)
[Tables](#)
[Figures](#)
[Back](#)
[Close](#)
[Full Screen / Esc](#)
[Printer-friendly Version](#)
[Interactive Discussion](#)